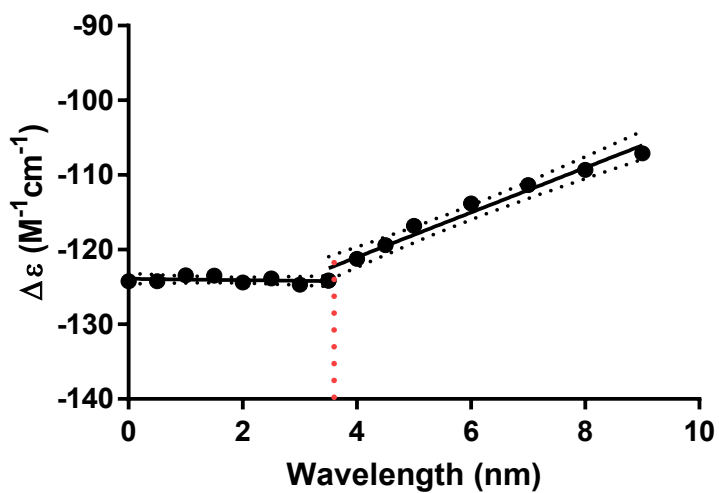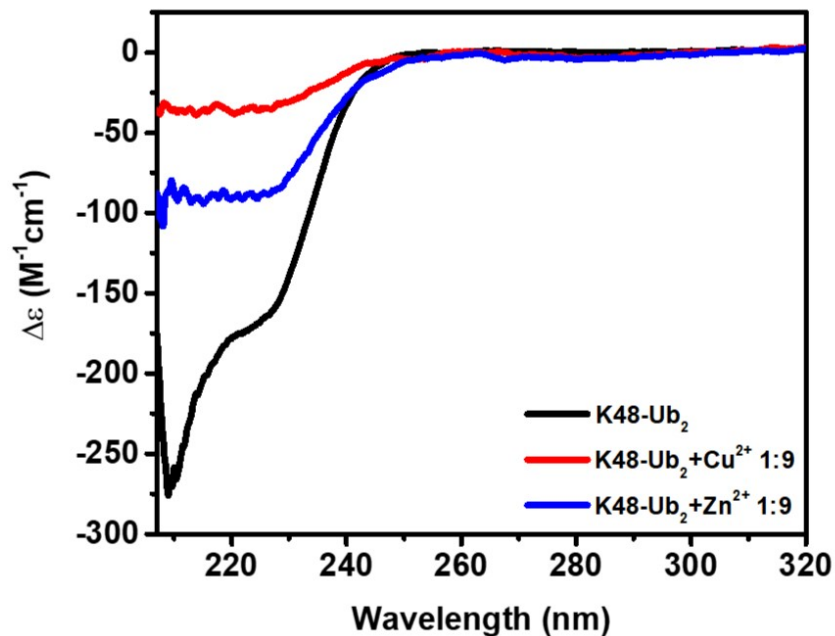## SUPPLEMENTARY INFORMATION



Figure S1. CD spectra changes of 6.8 µM K48-Ub$_2$ with Cu^{2+} binding curves, at λ=220 nm, M/P from 0:1 to 9:1 at room temperature. The values were analysed by FitSpline point-to-point and linear regression, 95% Confidence Intervals of the best-fit line were showed in dashed lines.

Figure S2 Far-UV CD spectra of 6.8 µM K48-Ub$_2$ (green line), K48-Ub$_2$/ Zn^{2+} (red line) and K48-Ub$_2$/ Cu^{2+} (blu line) (at 1:9 protein/metal ratios) , after a cycle of heating (up to 90°C) and cooling (down to 25°C).
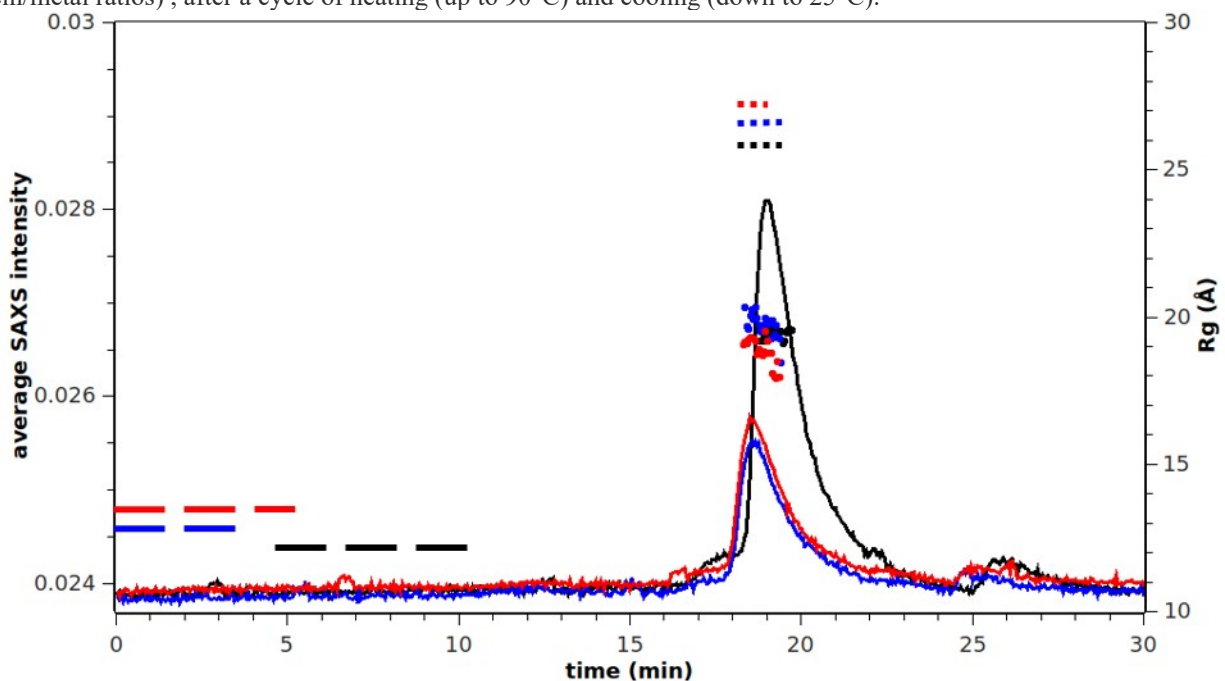
Figure S3 Averaged SAXS intensities versus elution time obtained by SEC-SAXS measurements for samples of K48-Ub$_2$ (black line), K48-Ub$_2$/Zn (blue line) and K48-Ub$_2$/Cu (red line). Protein concentration is 4 mg/ml and the investigated protein:metal ion molar ratio is 1:4. Frames selected for signal and background are highlighted in short-step and large-step dashed lines, respectively. Radius of gyration (R_g) values calculated for each frame are shown as dots.
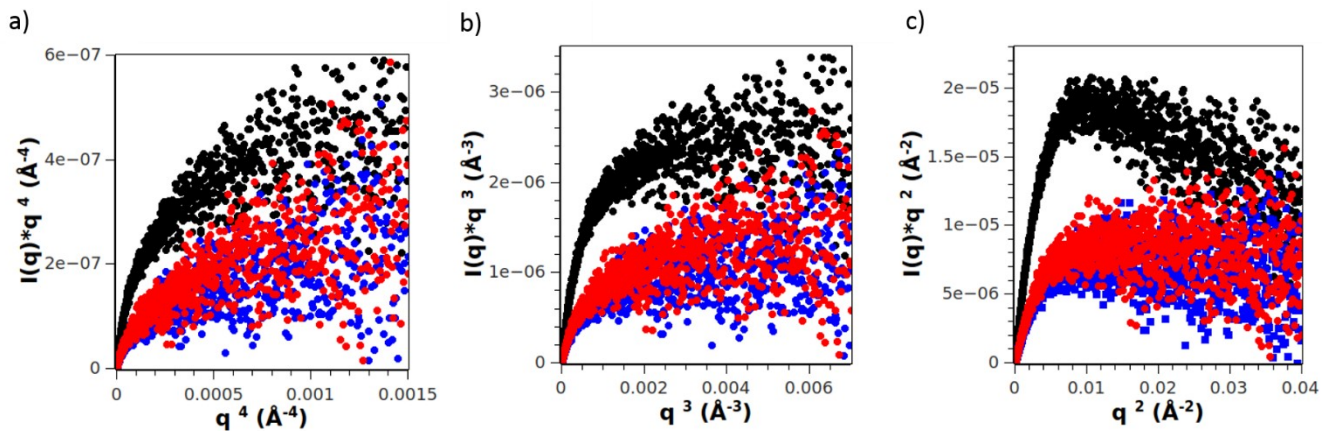
Figure S4. Flexibility analysis carried out by Porod-Debye (a), Sibyls (b), and Kratky-Debye (c) plots. K48-Ub$_2$ alone and in the presence of zinc and copper are shown as black, blue, and red dots, respectively.
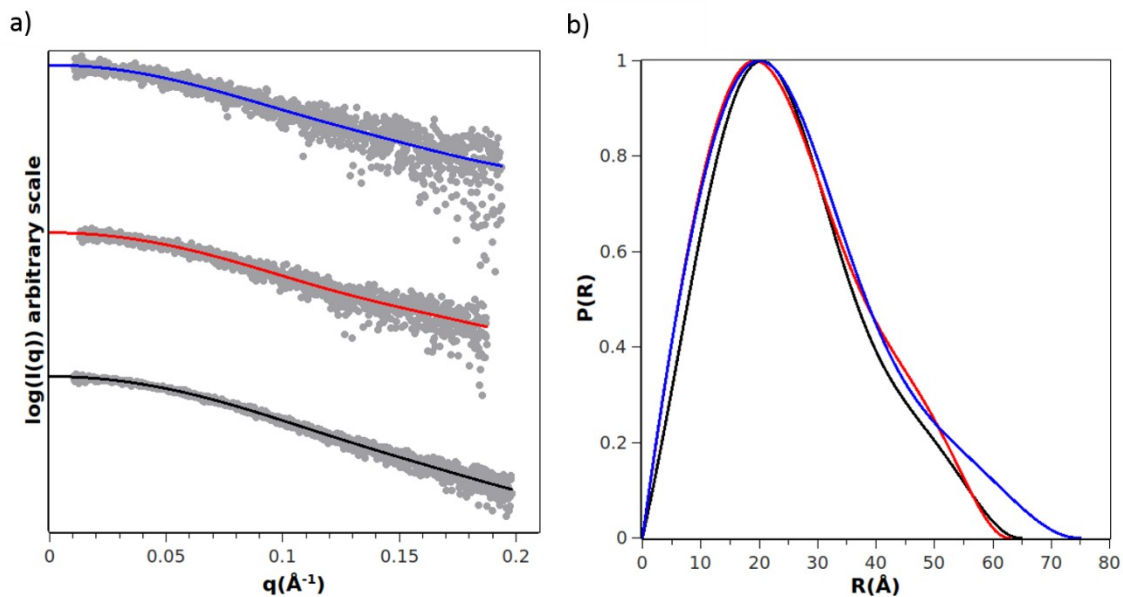
Figure S5. Results of the *P(R)* function determination from SAXS data in the reciprocal (a) and direct (b) space . Observed data are in grey color, *P(R)* functions and calculated data for K48-Ub$_2$ alone and in the presence of zinc and copper are shown as black, blue, and red lines, respectively.

.

About the use of symmetry in the molecular envelope generation

Because K48-Ub$_2$ is made by two identical copies of ubiquitin, we tested if SAXS data results from scattering objects characterized by two-fold symmetry. For each sample, 200 molecular envelopes were generated: 100 by applying two-fold symmetry restrain and 100 without symmetry restrain. The distributions of χ^2 values, parameter which represents the goodness of the fit between the scattering curve calculated from the envelope and the observed data, obtained in the presence and in the absence of restrain were compared by using a two-samples z-test (test performed by using the z_test_2 command included in Octave 4.0.3). The statistical significance α-value of 0.05 was set for the test. For each sample, the p-values obtained were greater than the α-value, pointing out that envelopes generated with and without symmetry are statistically comparable for such samples. Such result is a clear indication that SAXS data results from two-fold symmetry shaped objects because the modelling procedure provides two-fold symmetric models also in the case no symmetry restrains are used.
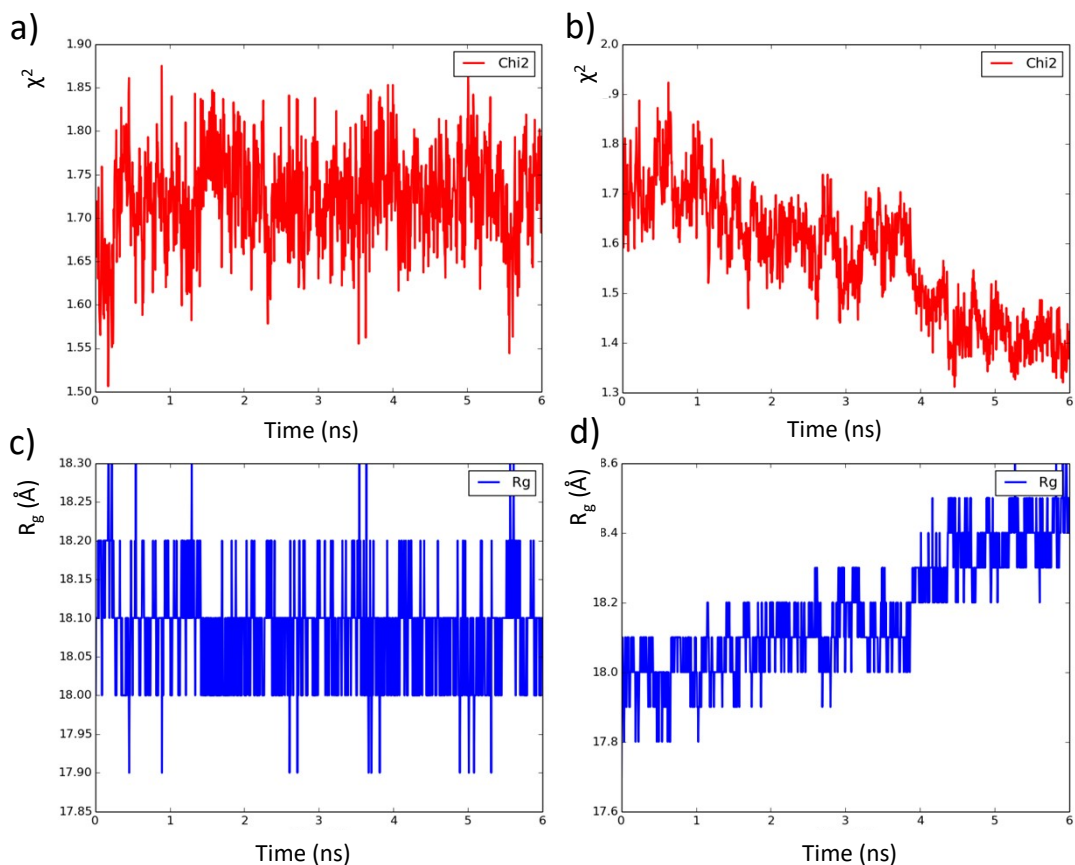
Figure S6. Results of molecular dynamics restrained by the experimental molecular envelopes, applied to K48-Ub$_2$, by using the crystal structure in open conformation (PDB code 3aul) (a,c) and in closed conformation (PDB code 1aar) (b,d). χ^2 value of the fit between calculated and observed SAXS profile (a,b) and radius of gyration R_g (c,d) as a function of the simulation time.
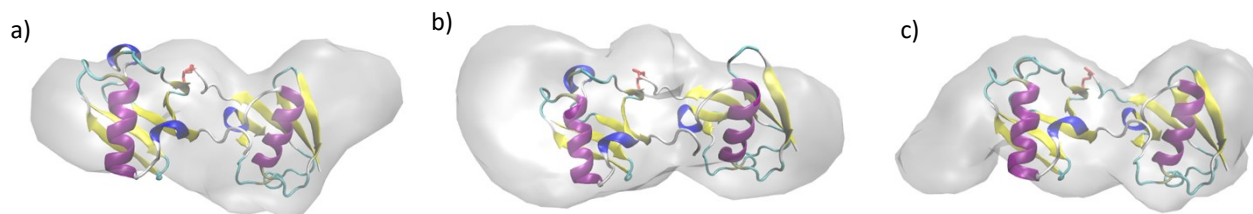


Figure S7. Results of the molecular dynamics carried out by using the MDFF protocol K48-Ub$_2$ alone (a), in the presence of zinc (b) and in the presence of copper (c). Final structural models superposed to the experimental molecular envelopes obtained by the DENSS program. The structural models are colored according to the secondary structure elements, with the K48-G76 bond shown in red.

Table S1. List of experimental structural models available for K48-Ub$_2$. MX=X-ray diffraction. The proximal and distal chains contain the ubiquitin units which contribute with K48 and G76, respectively, to the amide bond forming the ubiquitin dimer.

| PDB code	Technique	Proximal chain	Distal chain	Other molecules	Comment
1aar	MX	B	A		Closed conformation
3aul	MX	B	A		Open conformation
3m3j	MX	B	A		Closed conformation
3ns8	MX	B	A		Open conformation
5emz	MX	B	AE	Other 4 ubiquitin units (chains A,B,C,D)	Closed conformation, F45W mutation in the distal unit
5mn9	MX	B	A	Ubiquitin carboxyl-terminal hydrolase MINDY-1	Open conformation
6if1	MX	D	C	Ubiquitin-conjugating enzyme E2 K (chains A,B)	Open conformation
6tuv	MX	H	D	Ubiquitin carboxyl-terminal hydrolase MINDY-1 (chain A)	Open conformation
6z7v	MX	H	D	Ubiquitin carboxyl-terminal hydrolase MINDY-1 (chain A)	Open conformation, Mindy1 mutant P138A
6txb	MX	H	D	Ubiquitin carboxyl-terminal hydrolase MINDY-1 (chain A)	Open conformation, Mindy1 mutant P138A
7s6o	MX	B	A		Open conformation
2bgf	NMR	A	B		10 conformers
2kde	NMR	C	B	26S proteasome non-ATPase regulatory subunit 4 (chain A)	7 conformers, major S5a
2kdf	NMR	C	B	26S proteasome non-ATPase regulatory subunit 4 (chain A)	7 conformers, minor S5a
2n3v	NMR	B	C	26S proteasome regulatory subunit RPN1 (chain A)	10 conformers, extended binding mode
2n3w	NMR	B	C	26S proteasome regulatory	10 conformers, contracted binding

				subunit RPN1 (chain A)	mode
2lvp	NMR	B	A	E3 ubiquitin-protein ligase AMFR (chain C)	20 conformers, gp78CUE domain bound to the distal ubiquitin
2lvq	NMR	B	A	E3 ubiquitin-protein ligase AMFR (chain C)	24 conformers, gp78CUE domain bound to the proximal ubiquitin
2pea	NMR	A	B		1 conformer, closed conformation, Experimental Global Rotational Diffusion Tensor from NMR Relaxation Measurements
2pe9	NMR	A	B		Open conformation, 1 conformer, Experimental Global Rotational Diffusion Tensor from NMR Relaxation Measurements
5ymy	NMR	A	B	Proteasomal ubiquitin receptor ADRM1 (chain C)	Open conformation, 20 conformers
6uyi	NMR	C	D	26S proteasome non-ATPase regulatory subunit 1 (chain D)	Open conformation, 15 conformers, bound to proximal unit
6uyj	NMR	C	D	26S proteasome non-ATPase regulatory subunit 1 (chain D)	Open conformation, 15 conformers, bound to distal unit
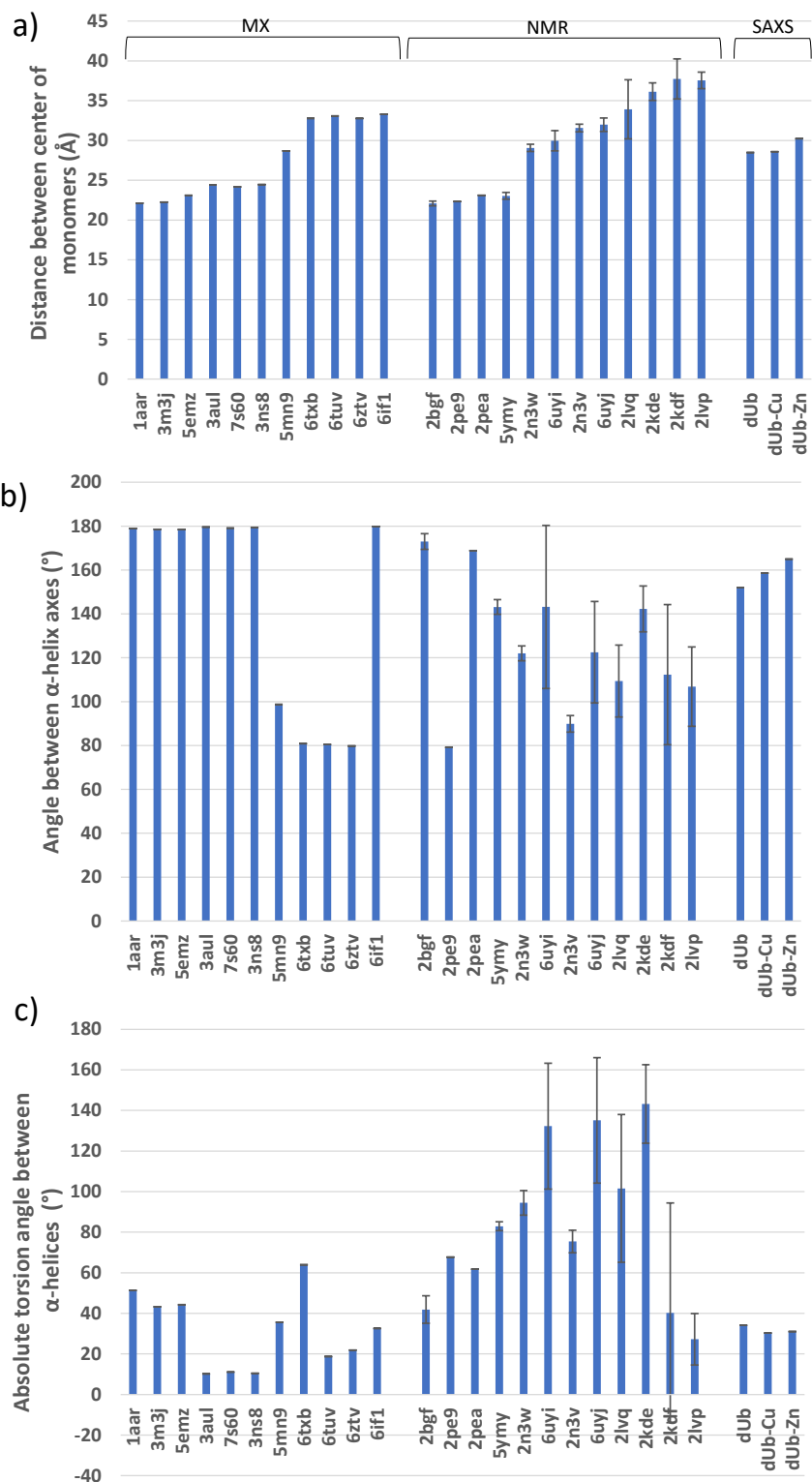
Figure S8. Comparison of experimental structural models of K48-Ub$_2$ obtained by MX, NMR and SAXS according to three geometrical descriptors characterizing the mutual location of the two monomers: the distance between the barycenters (a), the angle between the α-helices axes (b) and the absolute value of the torsion angle between the α-helices (c). Error bars in NMR structures take into account the variability among conformers. The structural models from a given technique have been sorted according to increasing values of the distance between the barycenters.

Further comments on Figure S9

As expected, the presence of an interacting protein leads to a larger separation of the ubiquitin monomers, regardless the technique used to obtain the structure (Figure S7a). Our SAXS structures show D values shorter than that observed in the presence of an interacting protein and larger than those observed in the absence of it. By considering crystal structures, the closed conformations show T values (~45°) higher than those determined for the open conformation (~10°) (Figure S9c). In the case of the structures in elongated open conformation, the D descriptor values range from ~20° to ~70°. Despite NMR-detected compact open conformation is not available and, thus, it is not possible to compare the values of the T descriptor of such conformation with the closed one in the case of the NMR structures, similitudes can be observed between NMR and crystal structures: i) the only two NMR structures showing closed conformation (2pea and 2bgf) have T values close to those of the closed conformation detected by X-ray diffraction and ii) the remaining NMR structures, which are featured by elongated open conformation, show variable T values (from ~30 to ~140°) as in the case of the elongated open conformations detected by X-ray diffraction. Regarding the A descriptor (Figure S9b), it appears not able to distinguish closed, compact open, and elongated conformation. It is worth noting that the variability observed for the T and A values of the elongated open conformations is expected because such conformations are not restrained by inter-chain interactions and, hence, sample a large conformational space. Interestingly, although our SAXS structures show elongated open conformation, their T and A values have limited variations.
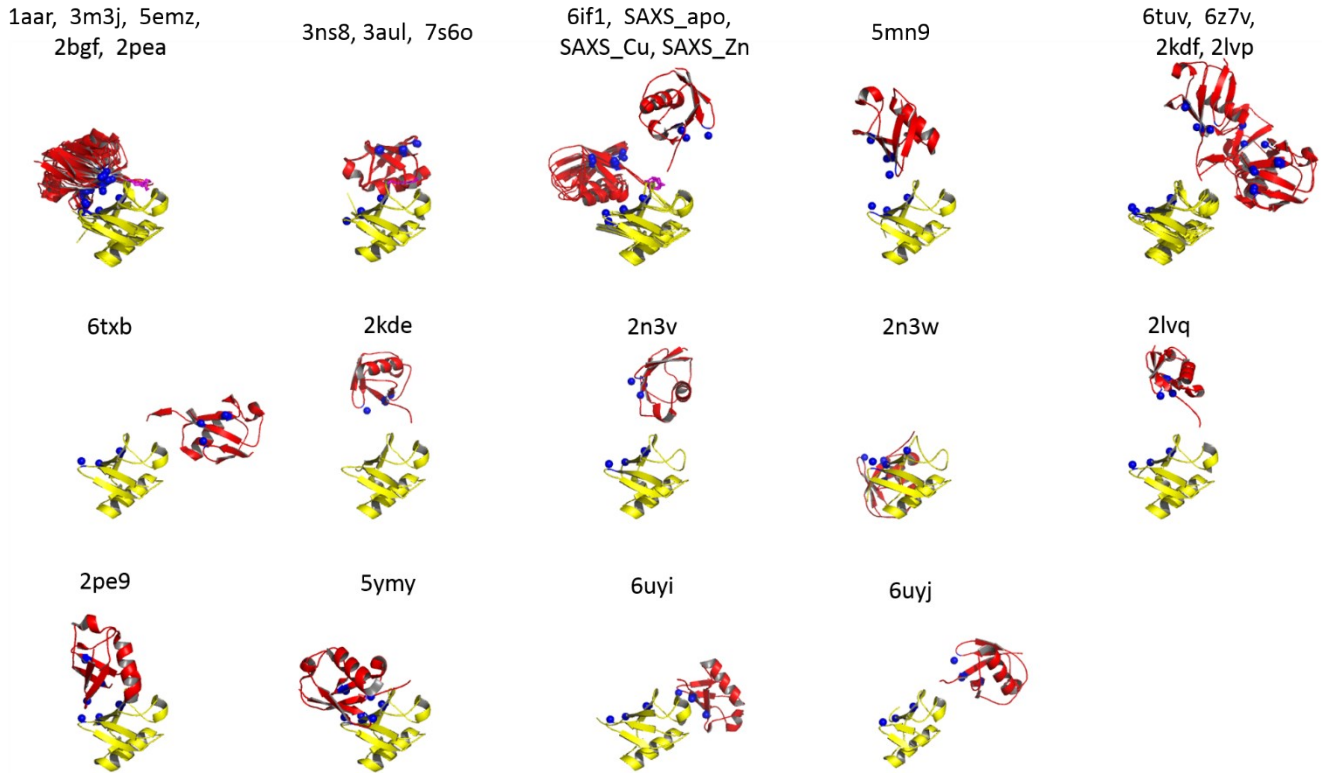
Figure S9 Comparison of K48-Ub$_2$ structures. The figure includes structures deposited in the PDB and obtained by X-ray diffraction or NMR and our structure obtained by SAXS (SAXS_apo, SAXS_Cu, SAXS_Zn). In the case of NMR structures, the figure shows the result of model averaging performed by using the state_avg.py script of Pymol. The structures are grouped according to the result of PCA and clustering analysis (Figure R6a) and their proximal chain (yellow) is superposed to that of 1aar. The distal chain is in red and the C$_\alpha$ atoms of the residues involved in the hydrophobic inter-chain interaction (Val70, Ile44, Leu8) are shown as blue spheres. The residues involved in the diubiquitin covalent link, when present in the structure, are in magenta.